

## New Mechanism Synthesis of 1,4-Benzothiazine and its Inhibition Performance on Mild Steel in Hydrochloric Acid

S. Aloui,<sup>1</sup> I. Forsal,<sup>2,\*</sup> M. Sfaira,<sup>3</sup> M. Ebn Touhami,<sup>2</sup> M. Taleb,<sup>3</sup>  
M. Filali Baba,<sup>3</sup> M. Daoudi<sup>1</sup>

<sup>1</sup> *Laboratoire de Chimie Organique, Faculté des Sciences Dhar El Mahraz, BP 1796 Atlas, Fès – Morocco.*

<sup>2</sup> *Laboratoire d'Electrochimie, Corrosion et Environnement, Faculté des Sciences, BP 133, Kénitra – Morocco.*

<sup>3</sup> *Laboratoire d'Analyses Physico-chimiques et Matériaux Catalytiques pour l'Environnement, Faculté des Sciences Dhar El Mahraz, BP 1796 Atlas, Fès- Morocco.*

Received 13 May 2009; accepted 21 October 2009

---

### Abstract

1-(3-methyl-4H-1,4-benzothiazin-2-yl)ethanone (1,4-BT) was synthesised via a new mechanism. 1,4-BT was thereafter tested as corrosion inhibitor of mild steel in hydrochloric solution at 293 K by weight loss measurements and electrochemical techniques (potentiodynamic polarisation, polarisation resistance, impedance spectroscopy (EIS)). Inhibiting efficiency (E%) increased with concentration and reached highest values up to 98% even at low concentration with changing the mechanism of the corrosion process. Results obtained showed that the inhibitor studied was an efficient inhibitor, especially in cathodic domain. The temperature effect on the corrosion behaviour of mild steel in 1 M HCl with and without 1,4-BT at  $5 \cdot 10^{-3}$  M was studied in the temperature range from 293 to 333 K. E% remains the same even at high temperature. The adsorption free energy and activation parameters for the mild steel dissolution reaction, in the presence of 1,4-BT, were determined. 1,4-BT is adsorbed on the mild steel surface according to a Langmuir isotherm adsorption model.

**Keywords:** mild steel, corrosion inhibition, 1,4-benzothiazine, thermodynamic parameters.

---

### Introduction

The widespread use of mild steel in many industries is well-recognised. As a result of its industrial concern, attention has been paid to prevent this metal against corrosion in different media. The applications of mineral acids as

---

\* Corresponding author. E-mail address: forsallisam@yahoo.fr

aggressive solutions are numerous. The most important areas of application are acid pickling, oil well acidizing, acid cleaning and acid descaling, etc. Because of the general aggressiveness of acids, inhibitors are often used to control attack of acid environment and to reduce the overall corrosion current density. The inhibition effectiveness might be due to the formation of thin layers of metal-inhibitor complexes as Trabanelli and his co-workers reported [1]. Generally, the diminution of the corrosion rate is a result of adsorption which makes, in acidic media, an effective blocking of the active sites of metal dissolution and/or hydrogen evolution. The adsorption requires the existence of attractive forces between the adsorbate and the metal. The principal types of interaction between an organic inhibitor and metal surface are physisorption, chemisorption or both of them. The adsorption of inhibitor is influenced by the nature and surface charge of the metal, the type of aggressive electrolyte, temperature and the chemical structure of the inhibitor. Indeed, specific interaction between functional groups and the metal surface and heteroatoms like nitrogen, oxygen, sulphur and phosphorus play an important role in the inhibition process due to the free electron pairs they possess [2]. Compounds that contain  $\pi$ -bonds generally exhibit good inhibitive properties by supplying electrons via the  $\pi$  orbital. When both of these features combine, enhanced inhibition can be observed.

Several amines [3-5], aminothiols [6-8], thio-compounds [9-12], triazole [13-16], tetrazole [17-19], imidazole [20-22], thiazoles [23-24], phosphonate [25] and surfactants [26,27] exhibit good inhibitory effect in hydrochloric acid. Notwithstanding several structural similarities with some of the above mentioned compounds, the derivatives of benzothiazine have not been studied, in our knowledge, as steel corrosion inhibitors.

The present study was undertaken to investigate the mild steel corrosion inhibition in molar hydrochloric acid by 1-(3-methyl-4H-1,4-benzothiazin-2-yl)ethanone (denoted hereafter 1,4-BT). The study was conducted by weight loss, polarisation and impedance methods. The thermodynamic parameters of 1,4-BT molecule adsorption onto mild steel were determined and the nature of inhibitor adsorption process was also studied and discussed.

## Experimental procedure

### *Synthesis and characterization of 1,4-benzothiazine compound*

1,4-BT has already been synthesized as reported elsewhere [28] with a mixture of 2-aminobenzenethiol and hydrazine hydrate which was heated to 100 °C for 2-3 minutes before introducing the 1,3-dicarbonyl. In the present work, the same compound 1,4-BT was obtained via a facile synthesis as illustrated in Scheme 1. The compound 1-(3-methyl-4H-1,4-benzothiazin-2-yl)ethanone (**3**  $\equiv$  1,4-BT) was prepared by direct condensation of 2-aminothiophenol 5g (40 mmol) with penta-2,4-dione 2g (20 mmol) in boiling ethanol as solvent, during four hours. After crystallization in ethanol, we obtained simultaneously a red crystal of **3** (5g, 60%) and trace of a yellow crystal **4** which were easily separated. The purity of

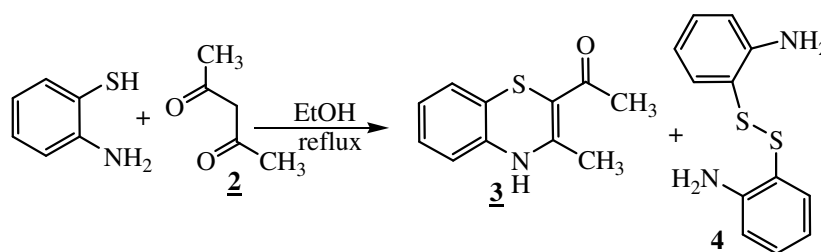
1,4-BT compound was checked by IR,  $^1\text{H}$  NMR,  $^{13}\text{C}$  NMR spectroscopy and mass spectra before use. The spectral characteristics of 1,4-BT are as follows: IR (KBr)  $\nu\text{ cm}^{-1}$ : 3277 (NH, s); 3194; 2925; 1602 (C=O, s), 1558-1494, 1460, 1429.

$^1\text{H}$  NMR (300 MHz, DMSO)  $\delta$  ppm: (s, 1H, NH), 7.19-6.62 (m, 4H, aromatic), 2.38 (s, 3H,  $\text{CH}_3$ ), 2.32 (s, 3H,  $\text{CH}_3$ ).

$^{13}\text{C}$  NMR (300 MHz, DMSO)  $\delta$  ppm: 193.38, 152.39, 131.46, 127.24, 126.8, 125.25, 120.11, 116.77, 114.71, 29.6, 22.33.

Mass spectrum: MS (EI)  $m/z$ :  $[\text{M}]^+$  = 205(86%); 176; 190; 162(100%); 130; 118; 109; 102; 91; 77; 65; 59.

1,4-BT was well dissolved in aqueous hydrochloric acid solutions and its structure is given in Scheme 1 (melting point m. p. = 192 °C, molecular weight  $M = 205\text{ g mol}^{-1}$ , frontal rapport  $R_f = 0.49$  (ether/hexane: 2/3)).



**Scheme 1.** New mechanism synthesis of **3**  $\equiv$  1,4-BT.

### **Gravimetric, steady-state and EIS measurements**

Prior to all measurements, the mild steel samples (0.03% P, 0.4% Mn, 0.08% C, 0.03% S and balance iron) were mechanically polished on wet SiC paper successively from 400 to 1200 grade. The specimens were washed thoroughly with bi-distilled water, decreased ultrasonically in ethanol and finally dried with acetone at room temperature before being immersed in the acid solution. The aggressive medium (1 M HCl) was prepared by dilution of analytical grade 37% HCl, and appropriate concentrations of 1,4-BT were obtained with doubly distilled water addition.

Gravimetric experiments were carried out in double-walled glass cell. The solution volume was 100 mL. The mild steel specimens used had rectangular form (1 cm  $\times$  5 cm  $\times$  0.08 cm). The immersion time for the weight loss was 24 h at  $293 \pm 1\text{ K}$ . After the corrosion test, the specimens were carefully washed in double distilled water, dried and then weighted. The rinse removed loose segments of corroded samples film. Triplicate experiments were performed in each case, and the mean value of the weight loss is reported. Weight loss allowed us to calculate the mean corrosion rate as expressed in  $\text{mg cm}^{-2}\text{ h}^{-1}$ .

Electrochemical measurements were investigated in a conventional three-electrode electrolysis cylindrical Pyrex glass cell equipped with thermostat-cooling condenser. The working electrode (WE), in the form of a disc cut from steel, had a geometrical area of  $1\text{ cm}^2$  and was embedded in polytetrafluoroethylene (PTFE) to avoid any infiltration of electrolyte. A saturated calomel electrode (SCE) and platinum electrode were used as reference

and auxiliary electrode, respectively. The temperature was thermostatically controlled at 293 K.

The polarisation curves were recorded with a digital potentiostat type Voltalab PGZ 100 and controlled with analysis software (Voltmaster 4), at scan rate of  $1 \text{ mV s}^{-1}$ . The mild steel electrode was maintained at open circuit conditions (corrosion potential,  $E_{\text{corr}}$ ) for 30 min and thereafter pre-polarized at  $-800 \text{ mV}$  for 10 min. After this scan, the potential was swept to anodic potentials.

The electrochemical impedance spectroscopy (EIS) measurements were performed using a transfer function analyser (Voltalab PGZ 100), with a small amplitude a.c. signal ( $10 \text{ mV rms}$ ) over a frequency domain from  $100 \text{ kHz}$  to  $10 \text{ mHz}$  at  $293 \text{ K}$  with 5 points per decade. Computer programs automatically controlled the measurements performed at rest potentials after 30 min of immersion at  $E_{\text{corr}}$ . The impedance diagrams were given in the Nyquist representation. In order to ensure reproducibility, all experiments were repeated three times. The evaluated accuracy was within 10%.

## Results and discussion

### Weight loss tests

Gravimetric measurements of mild steel were investigated in  $1 \text{ M HCl}$  in the presence and absence of various concentrations of 1,4-BT during 24 h of immersion period at  $293 \text{ K}$ . The mass loss is determined after removing the corrosion products from the metal solution in accordance to the ASTM G1-67. The values of the corrosion rate ( $W_{\text{corr}}$ ) and inhibiting efficiency ( $E_{\text{W}}\%$ ) are given in Table 1.  $E_{\text{W}}\%$  was estimated by the following relation (1):

$$E_{\text{W}}(\%) = \frac{W_{\text{corr}} - W_{\text{corr}/\text{inh}}}{W_{\text{corr}}} \times 100 \quad (1)$$

$W_{\text{corr}}$  and  $W_{\text{corr}/\text{inh}}$  are the corrosion rate of steel without and with inhibitor, respectively.

**Table 1.** Gravimetric results of the mild steel corrosion with and without addition of 1,4-BT molecule studied at  $293 \text{ K}$  after 24 h of immersion in  $1 \text{ M HCl}$ .

Inhibitor	Concentration ( $\text{mol L}^{-1}$ )	$W_{\text{corr}}$ ( $\text{mg cm}^{-2} \text{ h}^{-1}$ )	$E_{\text{W}}\%$
Blank	0	1.836	-
1,4-BT	$5 \times 10^{-5}$	0.097	94
	$1 \times 10^{-4}$	0.027	98
	$5 \times 10^{-4}$	0.010	99
	$1 \times 10^{-3}$	0.010	99

It is clear that the steel corrosion rate values decreases with the concentration of 1,4-BT, and in turn the inhibiting efficiency increases to reach 99% at  $5 \times 10^{-4} \text{ mol L}^{-1}$  of 1,4-BT. Its efficiency is already as high as 94% when only  $5 \times 10^{-5} \text{ mol L}^{-1}$  were present in the solution.

The protective properties of such compound are probably due to the interaction of  $\pi$  electrons of thiazine and phenyl rings as well as the presence of electron donor groups (S, N and O) through which the ability is easy to form bonds with transition metals such as mild steel. The sulphur atom provides a high electron density and it was found that  $E\%$  increases with electron density [7]. Indeed, Chetouani et al. [29,30] have reported the importance of sulphur atom in the drastic change of adsorption mechanism. Furthermore, Brandt et al. [31] reported that the sulphur atom represents the active centre of aliphatic sulphides in their interaction with the metal surface.

### Current-voltage characteristics

Curves obtained in the presence and absence of 1,4-BT inhibitor, after prepolarizing the electrode at its  $E_{\text{corr}}$  for 30 min, are shown in Fig. 1. The potential was swept stepwise from the most cathodic potential to the anodic direction. This avoided electrolyte pollution by dissolved iron. The current-potential plots recorded in the vicinity of  $E_{\text{corr}}$  give the corresponding polarisation resistance,  $R_p$ , of mild steel in 1 M HCl in the presence of various concentrations of 1,4-BT.

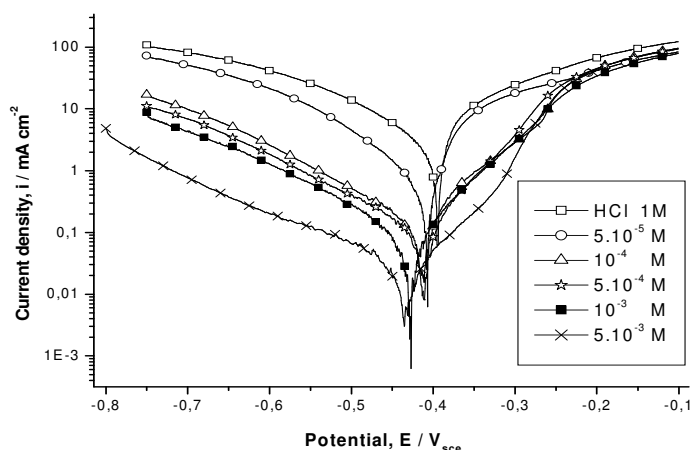


**Figure 1.** Polarization curves for mild steel in 1 M HCl containing different concentrations of 1,4-BT at 293 K.

Table 2 exemplifies the values of the associated electrochemical parameters (corrosion potentials ( $E_{\text{corr}}$ ), cathodic Tafel slopes ( $\beta_c$ ), corrosion current densities ( $i_{\text{corr}}$ ), polarisation resistances ( $R_p$ ) and inhibiting efficiencies ( $E_I\%$  and  $E_{R_p}\%$ )).

The following relations (2 and 3) determine  $E_I\%$  and  $E_{R_p}\%$ , respectively:

$$E_I\% = \frac{i_{\text{corr}} - i_{\text{corr}/\text{inh}}}{i_{\text{corr}}} \times 100 \quad (2)$$

$$E_{R_P} \% = \frac{R_P - R'_P}{R_P} \times 100 \quad (3)$$

where  $i_{\text{corr}}$  and  $i_{\text{corr/inh}}$  are the corrosion current density values without and with 1,4-BT, respectively determined by extrapolation of cathodic Tafel lines to the corrosion potential.  $R_P$  and  $R'_P$  are the polarisation resistances with and without 1,4-BT, respectively.

**Table 2.** Values of electrochemical parameters evaluated from the cathodic current-voltage characteristics for the system electrode / 1 M HCl with added inhibitor at 293 K.

Inhibitor	Concentration mol L <sup>-1</sup>	E <sub>corr</sub> mV <sub>sce</sub>	β <sub>c</sub>   mV dec <sup>-1</sup>	i <sub>corr</sub> μA cm <sup>-2</sup>	R <sub>P</sub> Ω cm <sup>2</sup>	E <sub>I</sub> %	E <sub>R<sub>P</sub></sub> %	θ
Blank	0	-396	125	1072	10	-	-	-
1,4-BT	5 × 10 <sup>-5</sup>	-408	123	343	49	68	79	0.68
	1 × 10 <sup>-4</sup>	-412	177	122	398	88	97	0.88
	5 × 10 <sup>-4</sup>	-413	167	56	420	94	97	0.94
	1 × 10 <sup>-3</sup>	-429	134	41	537	96	98	0.96
	5 × 10 <sup>-3</sup>	-436	153	9	620	99	98	0.99

From these data, it is clear that the increase of 1,4-BT concentration shifted the values of  $E_{\text{corr}}$  towards more cathodic potentials. Fig. 1 indicates that the cathodic current-potential curves give rise to Tafel lines, indicating that the hydrogen evolution reaction is activation controlled. In contrast, the anodic curves show that the inhibition mode of organic compound depends upon electrode potential. Indeed, for an overvoltage higher than  $-250 \text{ mV}_{\text{sce}}$ , the presence of 1,4-BT does not change the current-potential characteristics which means that the significant steel dissolution dominates the adsorption of the inhibiting film. Therefore, in the vicinity of  $E_{\text{corr}}$  and below  $-250 \text{ mV}_{\text{sce}}$  to more cathodic potentials, the increase of 1,4-BT concentration leads to a decrease in the current-density. Thus 1,4-BT acts as mixed inhibitor. In this case, the adsorption rate of 1,4-BT remains higher than its desorption rate. The inhibitor influences then the anodic reaction at potentials more negative than  $-250 \text{ mV}_{\text{sce}}$ . This phenomenon may be due to the desorption of 1,4-BT on the electrode [32,33]. For potentials more than  $-250 \text{ mV}_{\text{sce}}$ , both the anodic and cathodic current densities were decreased, thus 1,4-BT suppressed both the anodic and cathodic reactions, although mainly the cathodic one. It can also be seen from the experimental results that 1,4-BT decreased  $i_{\text{corr}}$ , and in contrast enhanced  $R_P$  significantly at all the studies concentrations.  $E_{R_P} \%$  and  $E_I \%$  are in good agreement and indicate the excellent effect of 1,4-BT as corrosion inhibitor of mild steel in 1 M HCl medium. It is to be noted that the Tafel slope in uninhibited medium is very compared to the theoretical value given in the literature [34]. The changed Tafel slopes ( $\beta_c$ ) in the presence of 1,4-BT indicate that the inhibitor acted by merely blocking the reaction sites of the metal surface with changing the cathodic reaction mechanism of hydrogen discharge.

### Results of EIS measurements

A better understanding of the mechanism taking place at the electrode surface was attained through EIS measurements. The EIS impedance was performed under potentiostatic conditions at  $E_{\text{corr}}$  in the uninhibited and inhibited acidic solution containing various concentrations of 1,4-BT. Before each measurement, the electrode was left at the open circuit conditions during 30 min. The electrode system did not evolve significantly during the impedance measurements. The impedance diagrams obtained are characterized by a capacitive behaviour (Fig. 2).

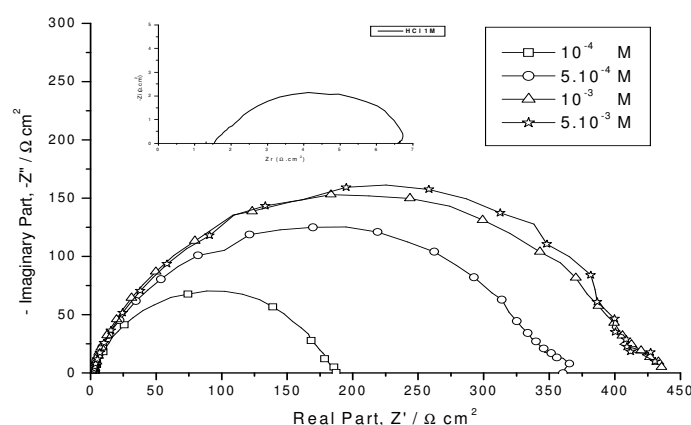


**Figure 2.** Impedance diagrams under open circuit conditions for an immersion time of 30 min; mild steel in 1 M HCl containing different concentrations of inhibitor 1,4-BT and in the insert only 1 M HCl.

A depressed semicircle, as often obtained in acidic media [4,5,11] can be seen. The difference from theoretical results is generally attributed to Cole-Cole [35,36] and/or Cole-Davidson [37] representations inherent to frequency dispersion, generally attributed to the generation of microscopic roughness at the surface during the corrosion process [38,39]. The existence of single semicircle relates the presence of single charge-transfer process, which is unaffected by the presence of 1,4-BT. According to a classical method, the EIS spectra of Fig. 2 will be interpreted in terms of parallel  $R_t$ - $C_d$  circuit; i.e., one time constant  $\tau_t$ . Table 3 summarizes the impedance parameters and values of  $E_{R_t}$  %.

**Table 3.** EIS data of mild steel in 1M HCl containing different concentrations of 1,4-BT at 293 K.

Concentration mol L <sup>-1</sup>	$R_t$ $\Omega$ cm <sup>2</sup>	$f_{\text{max}}$ Hz	$C_d$ $\mu\text{F}$ cm <sup>-2</sup>	$E_{R_t}$ %
Blank	6	160	165	-
$1 \times 10^{-4}$	186	77	11	96
$5 \times 10^{-4}$	361	70	6.3	98
$1 \times 10^{-3}$	439	58	6.2	98
$5 \times 10^{-3}$	440	59	6.1	98

The electrolyte resistance  $R_s$  determined between reference and working electrodes can be obtained from the abscissa axis intercept of the semicircle at  $f \rightarrow \infty$ ,  $R_s = 1.5 \Omega \text{ cm}^2$  in all solutions studied. Whereas  $R_t$  is the charge-transfer resistance and  $C_d$  the double layer capacitance. The charge-transfer resistance  $R_t$  values are calculated from the difference in impedance at lower and higher frequencies, i.e. the diameter of the semicircle. In first approximation,  $C_d$  and the frequency  $f_{\text{max}}$  at which the imaginary component of the impedance is maximal ( $-Z''_{\text{max}}$ ) are found as represented in equation 4:

$$f(-Z''_{\text{max}}) = \frac{1}{2\pi\tau_t}, \text{ where } \tau_t = R_t C_d \quad (4)$$

It may be assumed, as an approximation that, either  $(R_t)^{-1}$  [40] or  $(C_d)^{-1}$  [41] parameters are directly related with the corrosion rate. The inhibiting efficiency got from the charge-transfer resistance is calculated as follow, eq. (5):

$$E_{R_t} \% = \frac{R_{t/\text{inh}} - R_t}{R_{t/\text{inh}}} \times 100 \quad (5)$$

where  $R_t$  and  $R_{t/\text{inh}}$  are the charge-transfer resistance values without and with inhibitor, respectively.

It can be expected that the  $R_t$  values increase with 1,4-BT concentrations and consequently the inhibition efficiency increases. This indicates that the charge-transfer process mainly controls the corrosion of mild steel. The values of double layer capacitance are brought down to the maximum extend in the presence of 1,4-BT and the decrease of  $C_d$  follows the order similar to that obtained for  $i_{\text{corr}}$  in this study. This result is in favour of selectively adsorption of 1,4-BT in specific places [42] and/or formation of complex onto the metal surface [4]. According to this inhibition mechanism 1,4-BT could be adsorbed at active points, thus causing the corrosion rate to drop. The values of  $E_{R_t} \%$  obtained from EIS measurements agree with those deducted from polarisation and gravimetric methods.

### ***Influence of immersion period***

Fig. 3 presents the effect of immersion time on the impedance spectra at the corrosion potential. The inhibitor concentration was set at  $5 \times 10^{-3} \text{ M}$ . The shape of these diagrams is very similar to that obtained when varying the inhibitor concentration. The effect of increasing immersion time on impedance spectra is characterised by the increasing size of the loop observed, reaching a maximum after 8 hours, then it seems to be fairly constant afterward. The charge-transfer resistance at  $5 \times 10^{-3} \text{ M}$  of 1,4-BT and 293 K (determined at the low frequency limit of the impedance spectrum) changes from  $440 \Omega \text{ cm}^2$  after 0.5 h to ca.  $500 \Omega \text{ cm}^2$  after 8 h immersion. At the same time, the capacitance values remain almost the same, ca.  $6 \mu\text{F cm}^{-2}$  in the presence of 1,4-BT. These results demonstrate that the formation of surface film, and therefore the inhibitor

adsorption, on the electrode surface is reinforced with immersion time and is relatively fast and completed within 8 h [14].

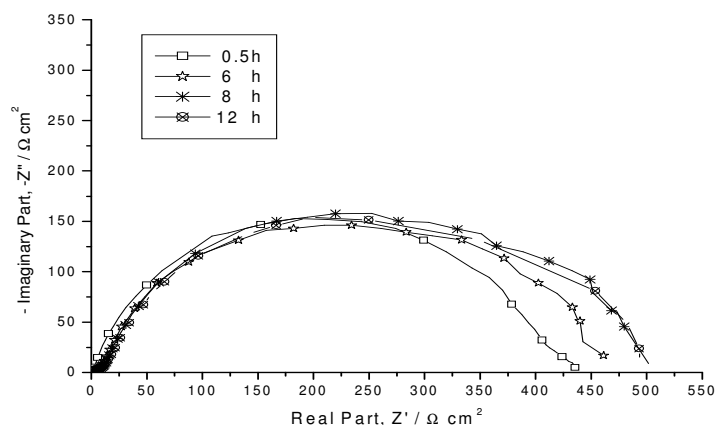


**Figure 3.** EIS spectra under open circuit conditions at different immersion times: system mild steel / 1 M HCl +  $5 \times 10^{-3}$  M of 1,4-BT at 293 K.

### Effect of temperature

We considered worthwhile to study the effect of temperature as it can modify the interaction between the mild steel electrode and the acidic medium in the presence and the absence of 1,4-BT. The interest in exploring the activation energy of the corrosion process and the thermodynamics of 1,4-BT adsorption was made by investigating the temperature dependence of the corrosion current densities using Tafel extrapolation method. Polarisation curves for mild steel in 1 M HCl without and with  $5 \times 10^{-3}$  mol L<sup>-1</sup> of 1,4-BT in the temperature range 293-333 K are shown in Fig. 4. The corresponding data are given in Table 4.

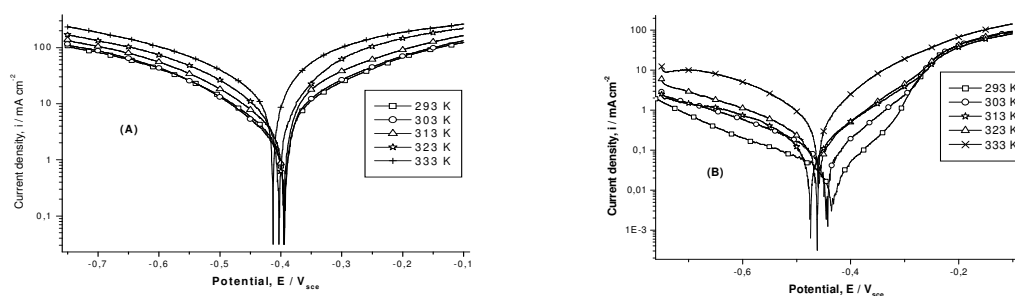


**Figure 4.** Effect of temperature on the cathodic and anodic responses for mild steel in (A) 1 M HCl and (B) 1 M HCl added of  $5 \times 10^{-3}$  M of 1,4-BT.

In the studied temperature range, the corrosion potential ( $E_{\text{corr}}$ ) and the Tafel slope ( $\beta_c$ ) are slightly modified in both uninhibited and inhibited media. The corrosion current density increases with the rise of temperature in both solutions and markedly pronounced in the absence of 1,4-BT. The values of inhibition efficiency remain nearly the same even at high temperature. These results

confirm that 1,4-BT acts as an efficient inhibitor in the range temperature from 293 to 333 K.

**Table 4.** Electrochemical characteristics of mild steel in 1 M HCl with and without  $5 \times 10^{-3}$  M of 1,4-BT at different temperatures.

	Temperature K	$E_{\text{corr}}$ mV <sub>sce</sub>	$i_{\text{corr}}$ $\mu\text{A cm}^{-2}$	$ \beta_c $ mV dec <sup>-1</sup>	$E_i$ %
Blank	293	-396	1072	125	-
	303	-395	2015	133	-
	313	-396	2158	140	-
	323	-404	2743	145	-
	333	-414	3420	181	-
1,4-BT	293	-436	9	153	99
	303	-445	32	145	98
	313	-463	46	131	98
	323	-476	55	134	98
	333	-461	77	137	98

The corrosion reaction can be regarded as an Arrhenius type process, the rate of which is given by equation (6) [43]:

$$i_{\text{corr}} = A \exp\left(-\frac{E_a}{RT}\right) \quad (6)$$

where A is the Arrhenius pre-exponential constant,  $E_a$  the apparent activation energy of the corrosion process, R the gas constant ( $R = 8.314 \text{ J K}^{-1} \text{ mol}^{-1}$ ) and T the absolute temperature.

Kinetic parameters, such as enthalpy and entropy of corrosion process, may be evaluated from the effect of temperature. An alternative formulation of Arrhenius equation, is called transition state [44], eq. (7):

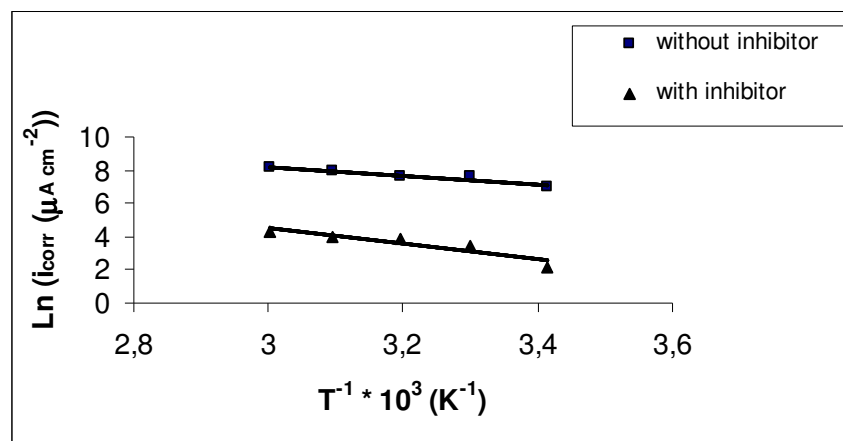
$$i_{\text{corr}} = \frac{k_B T}{h} \exp\left(\frac{\Delta S^*}{R}\right) \exp\left(-\frac{\Delta H^*}{RT}\right) \quad (7)$$

where  $k_B$  is the Boltzmann's constant ( $k_B = 1.38066 \cdot 10^{-23} \text{ J K}^{-1}$ ), h is the Planck's constant ( $h = 6.6252 \cdot 10^{-34} \text{ J s}$ ) and  $\Delta H^*$  and  $\Delta S^*$  are the enthalpy and the entropy of activation, respectively.

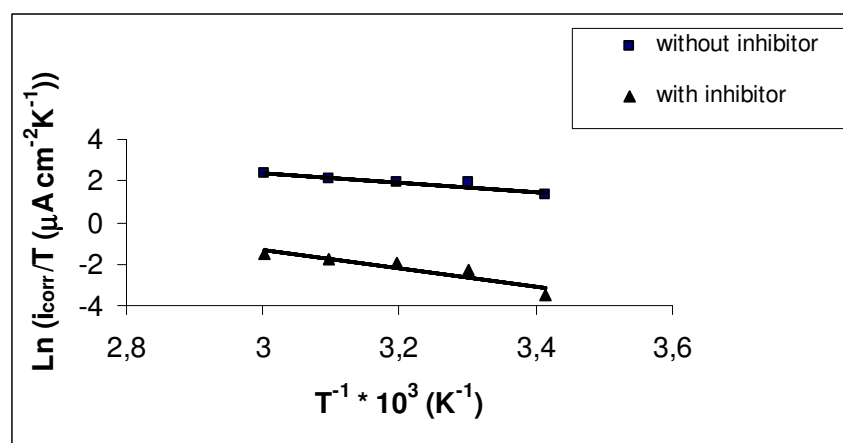
Fig. 5 presents the Arrhenius plots of the logarithm of the current density versus  $1/T$ , for mild steel in the corrosive medium with and without addition of  $5 \times 10^{-3}$  M of 1,4-BT. Straight lines are obtained with a slope of  $(-E_a/R)$ . Fig. 6 shows the plot of  $\text{Ln}(i_{\text{corr}}/T)$  against  $1/T$ . Straight lines are obtained with a slope of  $(-\Delta H^*/R)$  and an intercept of  $(\text{Ln } k_B/h + \Delta S^*/R)$ , which give the values of  $\Delta H^*$  and  $\Delta S^*$ .

Table 5 collects the values of activation parameters ( $E_a$ ,  $\Delta H^*$  and  $\Delta S^*$ ) for mild steel in the corrosive medium with and without addition of  $5 \times 10^{-3}$  of 1,4-BT.

Activation energy value obtained in the presence of 1,4-BT is ca. the double compared to that obtained from the inhibitor free 1 M HCl medium. Generally, the inhibitive additive causes rise in  $E_a$  value when compared to the blank and this could often be interpreted as an indication for the formation of an adsorptive film by a physical (electrostatic) mechanism [45] or chemisorption [46].



**Figure 5.** Arrhenius plots of mild steel in 1 M HCl with and without  $5 \times 10^{-3}$  M of 1,4-BT.



**Figure 6.** Arrhenius plots of  $\text{Ln}(i_{\text{corr}}/T)$  vs.  $1/T$  in 1 M HCl with and without  $5 \times 10^{-3}$  M of 1,4-BT.

**Table 5.** Values of activation parameters  $E_a$ ,  $\Delta H^*$  and  $\Delta S^*$  for mild steel in 1 M HCl and added of  $5 \times 10^{-3}$  M of 1,4-BT.

Concentration mol L <sup>-1</sup>	Pre-exponential factor, A $\mu\text{A cm}^{-2}$	$E_a$ kJ mol <sup>-1</sup>	$\Delta H^*$ kJ mol <sup>-1</sup>	$\Delta S^*$ J K <sup>-1</sup> mol <sup>-1</sup>
Blank	$8.327 \cdot 10^6$	21.48	18.88	-76.41
$5 \cdot 10^{-3}$	$1.563 \cdot 10^8$	39.73	37.13	-100.78

This high activation energy value supports the low value of  $i_{\text{corr}}$  deduced from the polarisation measurements and indicates the higher protective efficiency of 1,4-BT. In the same way, the pre-exponential factor A like  $E_a$  increases in the presence of 1,4-BT as reported by [47].

The positive values of  $\Delta H^*$  mean that the dissolution reaction is an endothermic process and that the dissolution of steel is difficult [48]. Practically  $E_a$  and  $\Delta H^*$

are of the same order. This result enabled us to check the thermodynamic relation of Gomma and Wahdan [49] between  $E_a$  and  $\Delta H^*$  as shown in eq. (8):

$$E_a - \Delta H^* = RT \quad (8)$$

The calculated value of the difference is  $2.6 \text{ kJ mol}^{-1}$  in the two solutions which is close to the experimental value of  $RT$ , ca.  $2.56 \text{ kJ mol}^{-1}$  at  $308 \text{ K}$ . Also the entropy  $\Delta S^*$  increases negatively in the presence of 1,4-BT than the non-inhibited one. This reflects the formation of an ordered stable layer of 1,4-BT onto the mild steel surface electrode [50]. The decrease of  $\Delta S^*$  in inhibited medium implies that the activation of 1,4-BT in the rate-determining step represents a dissociation rather than an association step, meaning that a decrease in disordering takes place on moving from reactants to activated complex [51].

### Adsorption isotherm

The adsorption isotherm provides useful insights into the mechanism of corrosion inhibition. The surface coverage,  $\theta$ , given in Table 2, was calculated according to equation 9:

$$\theta = \frac{i_{\text{corr}} - i_{\text{corr/inh}}}{i_{\text{corr}}} = \frac{E_I \%}{100} \quad (9)$$

Surface coverage values for the 1,4-BT were obtained from the current-voltage measurements at  $5 \times 10^{-3} \text{ M}$  of 1,4-BT at  $293 \text{ K}$ . Several adsorption isotherms were assessed. The best fitted straight line (Fig. 7) is obtained from the plot of  $C_{\text{inh}}/\theta$  versus  $C_{\text{inh}}$  with slope of 1.00564 around unity. The regression coefficient is  $r^2 = 0.99999$ . This suggests that the 1,4-BT adsorption on the metal surface obeyed to the Langmuir's adsorption isotherm, eq. 10 [52].

$$\frac{C_{\text{inh}}}{\theta} = \frac{1}{K_{\text{ads}}} + C_{\text{inh}}, \quad \text{with } K_{\text{ads}} = \frac{1}{55,55} \exp\left(-\frac{\Delta G_{\text{ads}}^\circ}{RT}\right) \quad (10)$$

where  $K_{\text{ads}}$  is the adsorption coefficient or adsorption equilibrium constant and  $\Delta G_{\text{ads}}^\circ$  is the standard free energy of adsorption. The calculated equilibrium constant of 1,4-BT adsorption reaction is 40404, which leads to  $\Delta G_{\text{ads}}^\circ = -37.45 \text{ kJ mol}^{-1}$ . The negative value of  $\Delta G_{\text{ads}}^\circ$  indicates the spontaneous adsorption of 1,4-BT on the steel surface [53]. More negative values of  $\Delta G_{\text{ads}}^\circ$  also suggest the strong interaction of 1,4-BT molecule onto the metal surface [54]. Then 1,4-BT inhibitor acts via chemisorption. Besides, this kind of isotherm which is generally regarded to indicate chemisorption [55], involves the assumption of no interaction between the adsorbed species on the electrode surface [56].

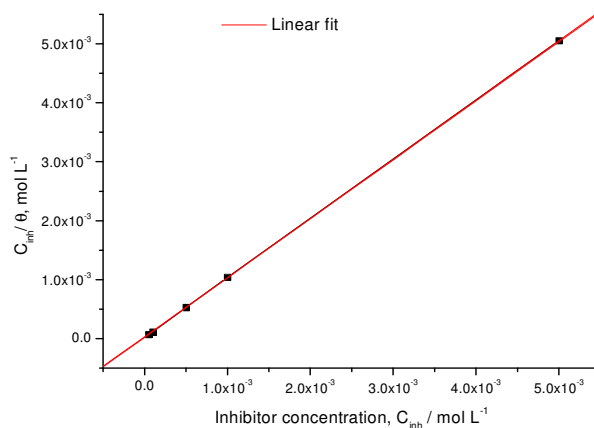


**Figure 7.** Langmuir adsorption isotherm plot for mild steel in 1 M HCl at different concentrations of 1,4-BT.

## Conclusion

The following main conclusions are drawn from the present study:

- \* 1-(3-methyl-4H-1,4-benzothiazin-2-yl)ethanone (1,4-BT) was obtained by a facile synthesis via a new mechanism.
- \* The results obtained showed the effectiveness of the investigated 1,4-BT molecule as an efficient inhibitor of mild steel in 1 M HCl.
- \* The inhibiting efficiency increases with concentration and remains as high as 98% even at high temperatures.
- \* 1,4-BT inhibitor acts as a mixed inhibitor.
- \* From all measurements carried out, the variation of inhibitive performance versus concentration shows the same trend.
- \* 1,4-BT adsorbs on the mild steel surface in 1 M HCl according to the Langmuir adsorption isotherm. The adsorption is spontaneous.

## References

1. M. Fonsati, F. Zucchi, G. Trabanelli, *Electrochim. Acta* 44 (1998) 311.
2. M. Hosseini, S.F.L. Mertens, M. Ghorbani, M.R. Arshadi, *Mater. Chem. Phys.* 78 (2003) 800.
3. A.L. de Queiroz Baddini, S.P. Cardoso, E. Hollauer, J.A. da Cunha Ponciano Gomes, *Electrochim. Acta* 53 (2007) 434.
4. A. Chetouani, M. Daoudi, B. Hammouti, T. Ben Hadda, M. Benkaddour, *Corros. Sci.* 48 (2006) 2987.
5. K. Tebbji, I. Bouabdellah, A. Aouniti, B. Hammouti, H. Oudda, M. Benkaddour, A. Ramdani, *Mater. Letters* 61 (2007) 799.
6. K.C. Pillali, R. Narayan, *Corros. Sci.* 23 (1983) 151.
7. B. Donnelly, T.C. Downie, R. Grzeskowiak, H.R. Hamburg, D. Short, *Corros. Sci.* 18 (1978) 109.

8. T. Sayerh, A. Srhiri, A. Ben Bachir, A. Sayagh, M. Chratbi, Proc. 7<sup>th</sup> Seic, Seliy, Ferrara, Italy 1 (1990) 241.
9. M.T. Makhlouf, S.A. El-Shatory, A. El-Said, *Mater. Chem. Phys.* 43 (1996) 76.
10. M. Elayyachi, B. Hammouti, A. El Idrissi, *Appl. Surf. Sci.* 249 (2005) 176.
11. M. Elayyachi, A. El Idrissi, B. Hammouti, *Corros. Sci.* 48 (2006) 2470.
12. M. Lebrini, M. Traisnel, M. Lagrenée, B. Mernari, F. Bentiss, *Corros. Sci.* 50 (2008) 473.
13. W. Li, Q. He, Ch. Pei and B. Hou, *Electrochim. Acta* 52 (2007) 6386.
14. El-S.M. Sherif, R.M. Erasmus, J.D. Comins, *J. Coll. Inter. Sci.* 311 (2007) 144.
15. H.H. Hassan, E. Abdelghani, M.A. Amin, *Electrochim. Acta* 52 (2007) 6359.
16. H.H. Hassan, *Electrochim. Acta* 53 (2007) 1722.
17. F. Zucchi, G. Trabaneli, M. Fonsati, *Corros. Sci.* 38 (1996) 2019.
18. H. Ma, T. Song, H. Sun, X. Li, *Thin Solid Films* 516 (2008) 1020.
19. M. Mihit, S. El Issami, M. Bouklah, L. Bazzi, B. Hammouti, E. Ait Addi, R. Salghi, S. Kertit, *Appl. Surf. Sci.* 252 (2006) 2389.
20. M. Scendo, M. Hepel, *Corros. Sci.* 49 (2007) 3381.
21. M. Scendo, M. Hepel, *J. Electroanal. Chem.* 613 (2008) 35.
22. L. Larabi, O. Benali, S.M. Mekelleche, Y. Harek, *Appl. Surf. Sci.* 253 (2006) 1371.
23. D. Kuron, H.-J. Rother, H. Graefen, *Werkst. Korros.* 32 (1981) 409.
24. O. Hollander, R.C. May, *Corrosion* 41 (1967) 39.
25. M. Benabdellah, A. Dafali, B. Hammouti, A. Aouniti, M. Rhomri, A. Raada, O. Senhaji, J.-J. Robin, *Chem. Eng. Comm.* 194 (2007) 1328.
26. S.-Z. Yao, X.-H. Jiang, L.-M. Zhou, Y.-J. Lv, X.-Q. Hu, *Mater. Chem. Phys.* 104 (2007) 301.
27. D. Chebabe, Z. Ait Chikh, A. Dermaj, K. Rhattas, T. Jasouli, N. Hajjaji, F. El Mdari, A. Srhiri, *Corros. Sci.* 46 (2004) 2701.
28. S.B. Munde, S.P. Bondge, V.E. Bhingolikar, R.A. Mane, *Green Chem.* 5 (2003) 278.
29. A. Chetouani, B. Hammouti, A. Aouniti, N. Benchat, T. Benhadda, *Prog. Org. Coat.* 45 (2002) 273.
30. A. Chetouani, A. Aouniti, B. Hammouti, N. Benchat, T. Benhadda, S. Kertit, *Corros. Sci.* 45 (2003) 1679.
31. H. Brandt, M. Fischer, K. Schawabe, *Corros. Sci.* 10 (1970) 631.
32. J. Wang, C. Cao, J. Chen, M. Zhang, G. Ye, H. Lin, *J. Chin. Soc. Corros. Protec.* 15 (1995) 241.
33. Y. Feng, K.S. Siow, W.K. Teo, A.K. Hsieh, *Corros. Sci.* 41 (1999) 829.
34. J.O'M. Bochriss, D. Drazic, *Electrochim. Acta* 7 (1962) 293.
35. K.S. Cole, R.H. Cole, *J. Chem. Phys.* 9 (1941) 341.
36. S. Duval, M. Keddam, M. Sfaira, A. Srhiri, H. Takenouti, *J. Electrochem. Soc.* 149 (2002) B520.
37. D.W. Davidson, R.H. Cole, *J. Chem. Phys.* 19 (1951) 1484.
38. K. Juttner, *Electrochim. Acta* 35 (1990) 1501.

39. F. Deflorain, V.B. Miscovic-Stankovic, P.L. Bonora, L. Fedrizzi, *Corrosion* 50 (1994) 446.
40. G. Gao, C.H. Liang, H. Wang, *Corros. Sci.* 49 (2007) 1833.
41. M. Lagrenée, B. Mernari, M. Bouanis, M. Traisnel, F. Bentiss, *Corros. Sci.* 44 (2004) 573.
42. J.M. Bastidas, J.L. Polo, E. Cano, C.L. Torres, *J. Mater. Sci.* 35 (2000) 2637.
43. I.N. Putilova, S.A. Balezin, V.P. Barannik, *Metallic Corrosion Inhibitors*, Pergamon Press, Oxford, 1960.
44. J.O'M. Bockris, A.K.N. Reddy, *Modern Electrochemistry*, vol. 2, Plenum Press, New York, 1977, pp. 1267.
45. A. Popova, E. Sokolova, S. Raicheva, M. Christov, *Corros. Sci.* 45 (2003) 33.
46. T. Szauer, A. Brandt, *Electrochim. Acta* 22 (1981) 1209.
47. G.N. Mu, X.M. Li, F. Li, *Mater. Chem. Phys.* 86 (2004) 59.
48. N.M. Guan, L. Xueming, L. Fei, *Mater. Chem. Phys.* 86 (2004) 59.
49. G.K. Gomma, M.H. Wahdan, *Mater. Chem. Phys.* 39 (1995) 209.
50. A. Yurt, A. Balaban, S.U. Kandemir, G. Bereket, B. Erk, *Mater. Chem. Phys.* 85 (2004) 420.
51. S. Martinez, I. Stern, *Appl. Surf. Sci.* 199 (2002) 83.
52. I. Langmuir, *J. Am. Chem. Soc.* 39 (1947) 1848.
53. J.D. Talati, D.K. Gandhi, *Corros. Sci.* 23 (1983) 1315.
54. L. Tang, X. Li, L. Li, Q. Qu, G. Mu, G. Liu, *Mater. Chem. Phys.* 94 (2005) 353.
55. Abo El-Khair, O.R. Khalifa, I.A. Abdelhamid, *Corros. Prevent. Contr.* 34 (1987) 1952.
56. A.J. Bard, L.R. Faulkner, *Electrochemical Methods*, John Wiley & Sons, New York, 1980, pp. 517.